Fluctuations and discrete particle noise in gyrokinetic simulation of drift waves

Thomas G. Jenkins and W. W. Lee
Princeton Plasma Physics Laboratory, Princeton, New Jersey 08543

(Received 24 August 2006; accepted 30 January 2007; published online 20 March 2007)

The relevance of the gyrokinetic fluctuation-dissipation theorem (FDT) to thermal equilibrium and nonequilibrium states of the gyrokinetic plasma is explored, with particular focus being given to the contribution of weakly damped normal modes to the fluctuation spectrum. It is found that the fluctuation energy carried in the normal modes exhibits the proper scaling with particle count (as predicted by the FDT in thermal equilibrium) even in the presence of drift waves, which grow linearly and attain a nonlinearly saturated steady state. This favorable scaling is preserved, and the saturation amplitude of the drift wave unaffected, for parameter regimes in which the normal modes become strongly damped and introduce a broad spectrum of discreteness-induced background noise in frequency space. © *2007 American Institute of Physics*. [DOI: 10.1063/1.2710808]

I. INTRODUCTION

The gyrokinetic model of a plasma, in addition to its original success[1,2] in analytically describing low-frequency phenomena (relative to the ion gyrofrequency) of moderate wavelength ($k_\perp \rho_i \sim 1$, where ρ_i is the ion gyroradius), has also been shown to be extremely well-suited for use in large-scale numerical simulations.[3,4] Recent particle-in-cell (PIC) simulations,[5] for instance, can use upwards of 30 billion particles on massively parallel machines, and are able to model the behavior of toroidal fusion plasmas at multiple-teraflop speeds. On more modest scales, gyrokinetic PIC simulations have been used to investigate turbulence spreading in shaped plasmas,[6] collisionless and collisional tearing modes,[7] and the effects of nonadiabatic electrons[8] on turbulent simulations. They have also been employed to study collisional damping of zonal flows,[9] ion temperature gradient-driven turbulence in toroidal geometry,[10] and the size scaling of transport parameters in turbulent plasmas.[11]

Recent discussion in the fusion simulation community has centered on the topic of "discrete particle noise" and the effects that such noise may have on the long-time transport predictions of turbulent gyrokinetic PIC simulations.[12,13] Physical effects (such as collisions) are indeed associated with the discrete nature of the particles in a plasma. The discrete particle noise under discussion here, however, occurs even in collisionless simulations; because PIC simulations represent moments of the plasma distribution function by appropriately Monte-Carlo sampling a collection of marker particles evolving in the phase space, sampling noise associated with this representation is always present (and is reduced in amplitude as more markers are used in the sampling).[14,15] In thermal equilibrium, where statistical fluctuations are linearly Landau damped, the fluctuation-dissipation theorem (FDT) quantifies this phenomenon, providing a simple relation between the fluctuation spectrum of the plasma and the number of sampling markers. Fundamentally, however, one is interested in nonequilibrium situations; we wish to determine to what degree this behavior [i.e., the straightforward reduction of statistical (or "discrete particle") noise as the number of markers is increased] holds true as the plasma is driven from thermal equilibrium. Consequently, in this work we focus on the self-consistent response of the plasma distribution function to both the statistical noise and the physical parameters of the problem (e.g., density gradients), examining the behavior of drift waves in a plasma slab (where the equilibrium state is straightforward) and utilizing simulation techniques based on finite-size marker particles[16] (eliminating the need to calculate the N^2 interparticle forces, through the modification of particle interactions inside a Debye sphere), the gyrokinetic PIC model[3] (removing the space charge waves and simplifying the gyromotion), and the δf method[17] (wherein only the deviation of the plasma from a known equilibrium is modeled via Monte-Carlo sampling).

As we previously alluded, the nature of discreteness-induced noise in the plasma is related to the behavior of the fluctuation spectrum $\langle \delta\phi\delta\phi\rangle(\mathbf{k},\omega)$. Consequently, we explore the behavior of the fluctuation spectrum as low-frequency drift waves drive the plasma from thermal equilibrium to a nonlinearly saturated steady state, examining the behavior of the spectrum as a function of particle count and giving particular attention to the contribution of the weakly damped normal modes of the plasma to this spectrum. These normal modes carry the bulk of the particle discreteness-induced noise in electrostatic gyrokinetic plasmas;[4,18,19] we explore the validity of this statement as parameters of the system change so that the normal modes are no longer well-defined (i.e., as the damping rate of the normal modes becomes large). Additionally, we present results (relevant to the general issue of the relationship between noise and signal in a PIC simulation treated in existing literature; see Refs. 16, 20, and 21) demonstrating that the effects of discreteness-induced noise on the long-time behavior of nonlinearly saturated drift waves can be minimized for reasonable simulation parameters under certain conditions.

Section II of this paper introduces the equations of the gyrokinetic model, and presents the gyrokinetic fluctuation-dissipation theorem (FDT). In Sec. III, we describe the normal modes of the gyrokinetic plasma, and explore the conditions under which they are well-defined. We demonstrate that our thermal equilibrium simulations are consistent with

gyrokinetic theory and that these simulations satisfy the gyrokinetic FDT. Section IV explains how the simulation methods used are generalized to include the possibility of a density gradient (leading to linear drift waves); a calculation describing the nonlinear saturation of these waves (expanding upon the work of Ref. 22) is also given. Section V describes the relevance of the gyrokinetic FDT to the nonequilibrium, nonlinearly saturated states of the gyrokinetic plasma, and presents simulation results showing the relationship of these states and the particle-discreteness-induced background noise in the presence and absence of well-defined normal modes. We then conclude with some comments on the applicability of this work to the more general issue of the effect of noise in PIC simulations.

II. THE GYROKINETIC MODEL

A. Governing equations

In the limit of $k_\perp^2\rho_i^2 \ll 1$, the gyrokinetic Vlasov equation, which describes the phase space evolution of a gyrocenter distribution function $F_\alpha(\mathbf{x}, v_\parallel, t)$, can be written (in the absence of magnetic field gradients, and in the electrostatic limit) as

$$\frac{\partial F_\alpha}{\partial t} + v_\parallel \mathbf{b}\cdot\nabla F_\alpha - \nabla\phi\times\mathbf{b}\cdot\nabla F_\alpha - \frac{q_\alpha m_i}{q_i m_\alpha}\mathbf{b}\cdot\nabla\phi\frac{\partial F_\alpha}{\partial v_\parallel} = 0. \tag{1}$$

This equation, which resembles the drift kinetic equation, uses the conventional gyrokinetic normalization; lengths and times are normalized to the scaled gyroradius $\rho_s \equiv \sqrt{T_e/m_i}/\Omega_i$ and the inverse ion cyclotron frequency $\Omega_i^{-1} = (q_i B_0/m_i)^{-1}$, while the electrostatic potential ϕ is normalized to the electron temperature $T_e/|q_e|$. Here $\mathbf{b}$ is a unit vector in the direction of the (uniform) magnetic field $\mathbf{B} = B_0\mathbf{b}$, and $v_\parallel$ is a velocity coordinate parallel to this field. The charge, mass, and temperature of species α are represented by q_α, m_α, and T_α, respectively, and we assume that the ions are singly charged ($q_i = |q_e|$).

The gyrokinetic Poisson equation, in these normalized units, is given by

$$\nabla^2\phi\left(\frac{\lambda_{\mathrm{De}}^2}{\rho_s^2}\right) + \nabla_\perp^2\phi = -\sum_\alpha \frac{q_\alpha}{q_i}\int_{-\infty}^{\infty} F_\alpha dv_\parallel \tag{2}$$

with the first term on the left arising from the conventional Laplacian operator in Poisson's equation and the second term arising from the polarization charge.[3] Because the electron Debye length $\lambda_{\mathrm{De}} = (\epsilon_0 T_e/n_0 q_e^2)^{1/2}$ is much smaller than ρ_s, the first of these terms may be neglected. The dominance of the polarization term in Eq. (2) effectively changes the fundamental length scale of the gyrokinetic plasma from λ_{De} to ρ_s; we will later see this effect in examining the low-frequency limit of the gyrokinetic dielectric function.

For our slab model, we postulate a magnetic field in the $\mathbf{b} = \theta\hat{y} + \hat{z}$ direction (for some $\theta \ll 1$). We ignore variation in the $\hat{z}$ direction, and study the evolution of waves (perpendicular to the dominant field component) with discrete wave numbers $\mathbf{k} \equiv k_x l\hat{x} + k_y m\hat{y}$, for integer l and m, with $k_x \equiv 2\pi/L_x$ and $k_y \equiv 2\pi/L_y$. Here L_x and L_y are the dimensions of the slab (using periodic boundary conditions) in the $\hat{x}$ and $\hat{y}$ directions. We can then define a fundamental parallel wave number $k_\parallel \equiv \theta k_y$ and the perpendicular wave number $k_\perp(l,m) = \sqrt{k^2 - m^2 k_\parallel^2}$.

These equations are solved by the standard PIC methods, initially loading a set of particles with some reasonable initial conditions (in our case, a Maxwellian distribution in $v_\parallel$ and a uniform distribution in $\mathbf{x}$). We then iteratively evolve the positions of these particles according to the characteristics of the gyrokinetic Vlasov equation, interpolate their positions to a spatial grid, and calculate the electrostatic potential using Fourier transforms.

B. The fluctuation-dissipation theorem

In thermal equilibrium, where no spatial gradients are present, the linear dielectric function relevant to the physical system of Eqs. (1) and (2) can be written as

$$\mathcal{D}_{l,m}(\omega) = 1 + \frac{X_i + X_e}{k_\perp^2(l,m)}. \tag{3}$$

Here, $X_\alpha \equiv 1 + \xi_\alpha Z(\xi_\alpha)$, where $\xi_\alpha = \omega/\sqrt{2}mk_\parallel v_{t\alpha}$ and Z is the plasma dispersion function. The thermal velocity is given (because of the gyrokinetic normalization) by $v_{t\alpha} = \sqrt{m_i T_\alpha/m_\alpha T_e}$, and the dispersion relation can be obtained from the zeros of $\mathcal{D}_{l,m}(\omega)$. In the limit as $\omega \to 0$, the dielectric function (apart from a change of characteristic scale length $\lambda_{\mathrm{De}} \to \rho_s$) describes the familiar Debye shielding effect of kinetic theory.

The resemblance of Eqs. (1) and (2) to the conventional Vlasov-Poisson system suggests that many parallels can be drawn between gyrokinetic and conventional Vlasov theory, and Krommes *et al.*[19] have initially treated this topic (see also Ref. 23 for a lengthier discussion), formulating the classical fluctuation-dissipation theorem (FDT) for a gyrokinetic plasma in the electrostatic approximation. In the weakly coupled limit appropriate for collisionless plasma, the FDT describes the relationship between the plasma's fluctuation spectrum in thermal equilibrium and its linear (dissipative) response to an infinitesimal perturbation away from that equilibrium. One can formulate the latter quantity in terms of the plasma's linear dielectric function; according to the theorem, the thermal equilibrium fluctuation spectrum of our slab model satisfies

$$\langle \delta\phi\delta\phi\rangle_{l,m}(\omega) = \frac{2}{N\omega k_\perp^2(l,m)}\,\mathrm{Im}\left(1 - \frac{1}{\mathcal{D}_{l,m}(\omega)}\right). \tag{4}$$

Integration of this formula over all frequencies using residue theory, and normalizing to 2π, yields the fluctuation spectrum as a function of wave number only,

$$\langle \delta\phi\delta\phi\rangle_{l,m} = \frac{1}{T}\int_0^T \langle|\phi_{l,m}(t)|^2\rangle dt = \frac{1}{Nk_\perp^2(l,m)[1 + k_\perp^2(l,m)/2]}, \tag{5}$$

where T is the time over which the simulation runs [the left hand side being the time-averaged $|\phi_{l,m}(t)|^2$] and N is the

number of particles of a given species. The latter relationship is quite useful as a diagnostic of numerical simulations in thermal equilibrium (see Fig. 3 for an example) due to its ease of implementation.

III. NORMAL MODES

A. Theory

In certain cases,[24] the dominant contributions to the fluctuation spectrum of Eq. (4) come from only a few localized peaks at various values of ω in the spectrum. If we consider the case of normal modes (oscillations that damp on a time scale slow compared to the period of the wave), we can separate the real and imaginary parts of the dielectric function, $\mathcal{D}_{l,m}(\omega)=\mathcal{D}'_{l,m}(\omega)+i\mathcal{D}''_{l,m}(\omega)$, and obtain

$$\mathrm{Im}\left(1-\frac{1}{\mathcal{D}_{l,m}(\omega)}\right)=\left[\frac{\mathcal{D}''_{l,m}(\omega)}{\mathcal{D}'_{l,m}(\omega)^2+\mathcal{D}''_{l,m}(\omega)^2}\right]. \tag{6}$$

In the limit of small $\mathcal{D}''_{l,m}(\omega)$, which we expect from a normal mode, this Lorentzian form has the approximate form

$$\mathrm{Im}\left(1-\frac{1}{\mathcal{D}_{l,m}(\omega)}\right)\approx \pi\delta(\mathcal{D}'_{l,m}(\omega)) = \pi\sum_{p=1}^{p_0}\frac{\delta(\omega-\omega_p)}{(\partial\mathcal{D}'_{l,m}(\omega)/\partial\omega|_{\omega=\omega_p}}, \tag{7}$$

where we have assumed that there are p_0 normal modes [i.e., solutions of $\mathcal{D}'_{l,m}(\omega_p)=0$ for which the denominator is nonsingular]. Consequently, the approximate relation

$$\langle\delta\phi\delta\phi\rangle_{l,m}(\omega)=\frac{2\pi}{Nk_\perp^2(l,m)}\sum_{p=1}^{p_0}\frac{\delta(\omega-\omega_p)}{\omega(\partial\mathcal{D}'_{l,m}(\omega)/\partial\omega|_{\omega=\omega_p}} \tag{8}$$

holds, implying that the bulk of the fluctuation energy for a given wave number (as a function of ω) resides in localized peaks about the real frequencies of the normal modes, assuming such modes are reasonably well-defined.

The plasma described by the linear dielectric of Eq. (3) has two normal modes that are analogous (with appropriate changes of scaling) to the well-known Langmuir waves of conventional Vlasov theory in the long-wavelength limit; these modes are conventionally referred to as ω_H modes.[4] If we assume the ion and electron thermal velocities are small relative to the resonant phase velocity $\omega/k_\parallel$, we can expand $Z(\xi_\alpha)$ to obtain

$$\mathcal{D}'_{l,m}(\omega)\approx 1-\frac{\omega_H^2}{\omega^2};\quad \omega_H^2=\frac{m^2k_\parallel^2(v_{te}^2+v_{ti}^2)}{k_\perp^2(l,m)};\quad \omega_r=\pm|\omega_H|. \tag{9}$$

This gives the approximate result

$$\langle\delta\phi\delta\phi\rangle_{l,m}(\omega)|_{\text{large }\omega}\approx\frac{2\pi}{Nk_\perp^2(l,m)}\left[\frac{\delta(\omega-\omega_H)}{2}+\frac{\delta(\omega+\omega_H)}{2}\right] \tag{10}$$

for the fluctuation spectrum at high frequencies. However, the existence of these normal modes depends on the system size L_y through the parallel wave number $k_\parallel$; as the system size decreases, the resonant phase velocity moves from the tail of the initial Maxwellian distribution into the bulk of the distribution, the damping rate increases (as is the case for Langmuir waves, where the damping rate is proportional to the slope of the background distribution at the resonant velocity), and it is no longer meaningful to speak of the disturbance as a wave (it damps away on a time scale similar to the period of the real oscillation frequency). Additionally, the approximation of the Lorentzian of Eq. (6) as a delta function begins to fail; the distinct real frequency of a mode with long parallel wavelength is replaced by a band of frequencies near ω_p. Thus, for larger parallel wave numbers, the energy in the fluctuation spectrum cannot be said to reside in "normal modes;" rather, it resides in random fluctuations excited by the discrete nature of the particles in the plasma.

Ion acoustic modes may also be normal modes of Eq. (3); in the limit $\xi_e\ll 1,\xi_i\gg 1$; letting $\xi_e\sim 0$ and expanding $Z(\xi_i)$ to lowest nontrivial order yields

$$\mathcal{D}'_{l,m}(\omega)\approx\frac{[1-k_\perp^2(l,m)]}{k_\perp^2(l,m)}\left(1-\frac{\omega_{IA}^2}{\omega^2}\right);\quad \omega_{IA}^2=\frac{m^2k_\parallel^2v_{ti}^2}{[1+k_\perp^2(l,m)]};\quad \omega_r=\pm|\omega_{IA}| \tag{11}$$

for intermediate values of ω ($k_\parallel v_{ti}\ll\omega\ll k_\parallel v_{te}$). Although drift waves arise from the destabilization of ion acoustic modes by density gradients, in the thermal equilibrium case these modes are strongly Landau damped; their effects on the fluctuation spectrum are relatively unimportant if the ω_H modes are well-defined. The delta-function approximation (integrating only over intermediate values of ω) is consistent with this result; we obtain

$$\langle\delta\phi\delta\phi\rangle_{l,m}(\omega)|_{\text{int. }\omega}\approx\frac{2\pi}{N}\frac{1}{[1+k_\perp^2(l,m)]}\left[\frac{\delta(\omega-\omega_{IA})}{2}+\frac{\delta(\omega+\omega_{IA})}{2}\right]. \tag{12}$$

Since $k_\perp^2\ll 1$, the coefficient multiplying the delta functions is significantly smaller for these modes than the corresponding coefficient in Eq. (10).

It is known from Eq. (5) that integrating the exact fluctuation spectrum over all frequencies (normalized to 2π) yields the result

$$\langle\delta\phi\delta\phi\rangle_{l,m\text{ exact}}=\frac{1}{Nk_\perp^2(l,m)[1+k_\perp^2(l,m)/2]}=\frac{1}{Nk_\perp^2(l,m)}-\frac{1}{N[2+k_\perp^2(l,m)]} \tag{13}$$

which ought to be well-matched by the sum of the ω integrals over the approximate spectra we have derived in Eqs. (10) and (12). Performing these integrals and normalizing to 2π, we find that our procedure slightly overestimates the correct answer; we obtain

$$\langle \delta\phi\delta\phi\rangle_{l,m\ \text{approx.}} = \frac{1}{Nk_\perp^2(l,m)} + \frac{1}{N[1+k_\perp^2(l,m)]} \tag{14}$$

with the two terms arising from the ω_H modes and the ion acoustic modes, respectively. However, it is clear that the delta-function approximation is reasonable; the error is on the order of the relative contribution of the ion acoustic modes, which is small.

B. Numerical simulations

With our knowledge of the thermal equilibrium fluctuation spectra, we now verify that our code satisfies the fluctuation-dissipation theorem. We evolve particles along the characteristics of the gyrokinetic Vlasov equation, Eq. (1), obtaining

$$\frac{dx_{\alpha j}}{dt} = -\left(\frac{\partial\phi}{\partial y}\bigg|_{\mathbf{x}=\mathbf{x}_{\alpha j}}\right); \quad \frac{dy_{\alpha j}}{dt} = v_{\parallel\alpha j}\theta + \left(\frac{\partial\phi}{\partial x}\bigg|_{\mathbf{x}=\mathbf{x}_{\alpha j}}\right),$$

$$\frac{dv_{\parallel\alpha j}}{dt} = -\frac{q_\alpha m_i}{q_i m_\alpha}\theta\left(\frac{\partial\phi}{\partial y}\bigg|_{\mathbf{x}=\mathbf{x}_{\alpha j}}\right). \tag{15}$$

We also utilize the standard δf technique of setting $F_\alpha = F_{0\alpha} + \delta f_\alpha$ in Eq. (1); perturbations around the background Maxwellian $F_{0\alpha}$ are examined by defining the particle weight $w_\alpha \equiv \delta f_\alpha / F_\alpha$ and evolving the resulting weight equation

$$\frac{dw_{\alpha j}}{dt} = -(1-w_{\alpha j})v_{\parallel\alpha j}\theta\frac{q_\alpha}{q_i}\left(\frac{\partial\phi}{\partial y}\bigg|_{\mathbf{x}=\mathbf{x}_{\alpha j}}\right. \tag{16}$$

along with Eqs. (15). The appropriately weighted density perturbations are then interpolated to a grid and the potential found via Fourier transforms.

Numerically, one can also directly solve Eq. (3) and obtain a representation of Eq. (4) as a function of ω for a given (l,m). Normalizing this representation to $2\pi\langle\delta\phi\delta\phi\rangle_{l,m}$ [from Eq. (5)], we can then qualitatively compare the results with the predictions of Eqs. (10) and (12) and our simulations. As expected, we observe in Figs. 1 and 2 that the power does indeed reside in localized peaks that spread as the parallel wave number grows, and that the ion acoustic modes are relatively unimportant for small parallel wave numbers. Here we have used $L_x=32$, $\theta=0.01$, $(l,m)=(1,1)$, and $v_{te}^2 = m_i/m_e \approx 1837.0$ as L_y assumes the values $[30,23,16]$, yielding $k_\perp\rho_i=[0.08,0.11,0.19]$, respectively. The simulations use 128 grid points in both the x and y directions, along with $N=250\,000$ particles and a time step $\Delta t=0.1$. One notes that the positions of the peaks in ω are not well matched by our delta-function approximation; however, this can be rectified by retaining more terms in the expansion of the plasma dispersion functions (the algebra is unduly complicated and will not be included here). As previously mentioned, one can also see the degradation of the delta-function approximation of Eq. (7) (as well as the increasing contribution of the ion acoustic modes to the spectrum) as the parallel wave number is increased.

As noted by Hu and Krommes,[14] the use of the δf method requires us to normalize the potential fluctuations by a typical weight $\bar{w}$. For the ω_H modes, which [as the disparate velocities of Eq. (9) suggest] are predominantly supported by the electrons, the natural choice for $\bar{w}$ in this case is the root-mean-square electron weight $\sqrt{\Sigma_{j=1}^N w_{ej}(t)^2/N}$. We exhibit the simulation results, along with the theoretical curve obtained from Eq. (5) at lowest order, in Fig. 3. The simulation uses 128 grid points in the x and y directions, with $L_x=L_y=23$ and time step $\Delta t=0.125$. The parallel field component is given by $\theta=0.01$, and we have $T_e=T_i=1$ and $m_i/m_e=1837.0$. The agreement is quite good as one passes into the regime (relevant to meaningful Monte-Carlo sampling of the phase space) where an average of several marker particles of each species inhabit a grid cell; an average of one

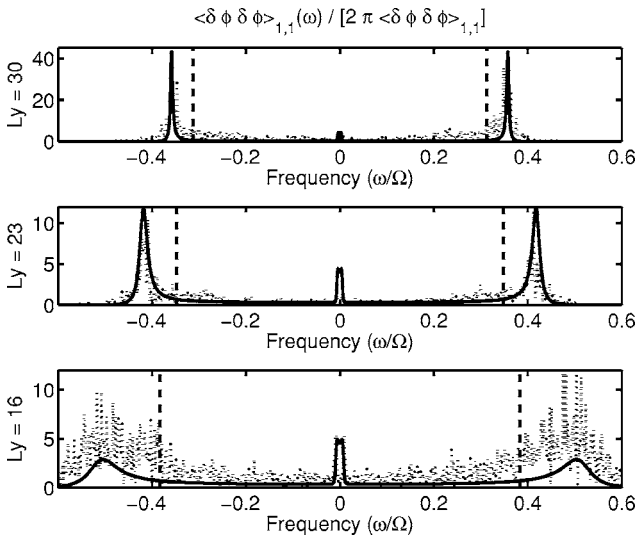

FIG. 1. The normalized fluctuation spectrum $\langle\delta\phi\delta\phi\rangle_{l,m}(\omega)/[2\pi\langle\delta\phi\delta\phi\rangle_{l,m}]$ for $(l,m)=(1,1)$ from the numerical solution of Eq. (4) (solid lines) and our simulation results (dotted lines) is plotted together with the delta-function approximation of Eq. (10) for the ω_H modes (dashed lines) as the parallel component of the wavelength is varied.

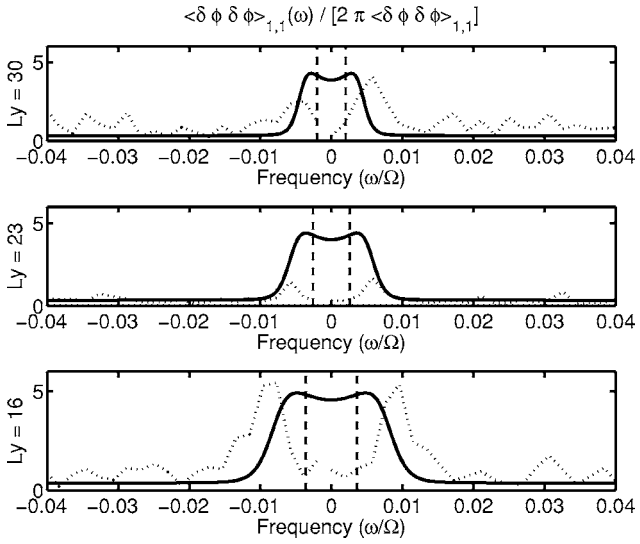

FIG. 2. The simulation results and theoretical predictions of Fig. 1, together with the delta-function approximation of Eq. (12) for the ion acoustic modes (dashed lines), are plotted over a narrower frequency range as the parallel component of the wavelength is varied.

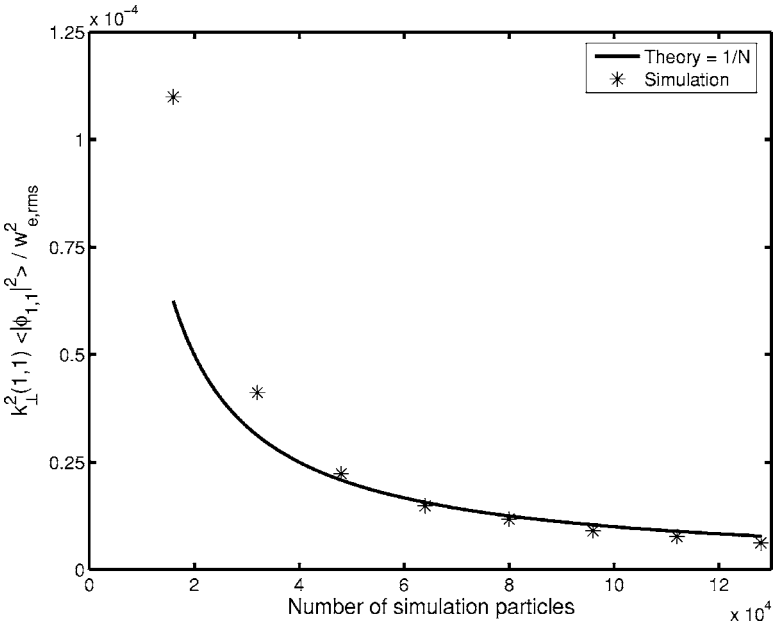

FIG. 3. Simulation results and theory exhibiting the scaling of the ω-integrated fluctuation spectrum with the number of simulation particles. The theoretical curve is obtained from Eq. (5) in the $k_\perp^2(l,m)\ll 1$ limit, with the potential normalized to the root-mean-square electron weight.

marker particle per species per grid cell occurs at the leftmost data point in the figure, where $N\sim 1.6\times 10^4$.

IV. DRIFT MODES

A. Linear growth

We now relax the constraint of thermal equilibrium by introducing a background density gradient that gives rise to drift waves. It is common[17,25,26] to impose a fixed background density gradient by modeling the particle density as an x-dependent function of a parameter κ_N, such that

$$\nabla F_{0\alpha} = -\kappa_N F_{0\alpha} \tag{17}$$

and neglecting this x -dependence where the gradient does not act specifically on $F_{0\alpha}$. Generally, we must have $|\kappa_N| < k_x$ for this procedure to be strictly valid (though this restriction is unnecessary for modes propagating perpendicular to the density gradient). With this assumption, the gyrokinetic Vlasov and Poisson equations (assuming equal temperatures for ions and electrons) can be written in the δf formalism as

$$\frac{\partial \delta f_\alpha}{\partial t} + v_\parallel \theta \frac{\partial \delta f_\alpha}{\partial y} + \kappa_N \frac{\partial \phi}{\partial y} F_{0\alpha} + v_\parallel \theta \frac{q_\alpha}{q_i}\frac{\partial \phi}{\partial y} F_{0\alpha} - \nabla \phi \times \hat{z}\cdot \nabla \delta f_\alpha - \frac{q_\alpha m_i}{q_i m_\alpha}\theta \frac{\partial \phi}{\partial y}\frac{\partial \delta f_\alpha}{\partial v_\parallel} = 0, \tag{18}$$

$$\nabla_\perp^2 \phi = -\sum_\alpha \frac{q_\alpha}{q_i}\int_{-\infty}^{\infty} \delta f_\alpha dv_\parallel. \tag{19}$$

We now make a standard assumption of quasilinear theory,[27] namely that (for real $\omega_{l,m}$,)

$$\phi(x,y,t) = \epsilon \sum_{l=-\infty}^{\infty}\sum_{m=-\infty}^{\infty} \hat{\phi}_{l,m}(\epsilon t) e^{ik_x l x} e^{ik_y m y} e^{-i\omega_{l,m} t}, \tag{20}$$

$$\delta f_\alpha(x,y,v_\parallel,t) = \epsilon \sum_{l=-\infty}^{\infty}\sum_{m=-\infty}^{\infty} \widehat{\delta f}_{\alpha,l,m}(v_\parallel,\epsilon t) e^{ik_x l x} e^{ik_y m y} e^{-i\omega_{l,m} t}, \tag{21}$$

where the quantities $\hat{\phi}_{l,m}(\epsilon t)$ and $\widehat{\delta f}_{\alpha,l,m}(v_\parallel,\epsilon t)$ vary slowly in time relative to the period $T=2\pi/\omega_{l,m}$, and the quantity $\epsilon=1$ is an ordering parameter denoting this slow variation. Defining $\omega_N^* \equiv k_y \kappa_N$, we then obtain

$$\frac{\partial}{\partial t}\widehat{\delta f}_{\alpha,l,m}(v_\parallel,\epsilon t) - i(\omega_{l,m} - m k_\parallel v_\parallel)\widehat{\delta f}_{\alpha,l,m}(v_\parallel,\epsilon t) + im\hat{\phi}_{l,m}(\epsilon t) F_{0\alpha}(v_\parallel)\left(\omega_N^* + \frac{q_\alpha}{q_i}k_\parallel v_\parallel\right) + \epsilon \sum_{l'=-\infty}^{\infty}\sum_{m'=-\infty}^{\infty} e^{i(\omega_{l,m}-\omega_{l',m'}-\omega_{l-l',m-m'})t}\left[k_x k_y (m' l - l' m) - im' k_\parallel \frac{q_\alpha m_i}{q_i m_\alpha}\frac{\partial}{\partial v_\parallel}\right]\hat{\phi}_{l',m'}(\epsilon t)\widehat{\delta f}_{\alpha,l-l',m-m'}(v_\parallel,\epsilon t) = 0, \tag{22}$$

$$k_\perp^2(l,m)\hat{\phi}_{l,m}(\epsilon t) = \sum_\alpha \frac{q_\alpha}{q_i}\int_{-\infty}^{\infty} \widehat{\delta f}_{\alpha,l,m}(v_\parallel,\epsilon t) dv_\parallel. \tag{23}$$

Ignoring the nonlinear $\hat{\phi}_{l',m'}(\epsilon t)\widehat{\delta f}_{\alpha,l-l',m-m'}(v_\parallel,\epsilon t)$ terms allows us to solve the Vlasov equation,

$$\widehat{\delta f}_{\alpha,l,m}(v_\parallel,\epsilon t) = \widehat{\delta f}_{\alpha,l,m}(v_\parallel,0) e^{i(\omega_{l,m}-m k_\parallel v_\parallel)t} - imF_{0\alpha}(v_\parallel)\left(\omega_N^* + \frac{q_\alpha}{q_i}k_\parallel v_\parallel\right) \times \int_0^t \hat{\phi}_{l,m}[\epsilon(t-\lambda)] e^{i(\omega_{l,m}-m k_\parallel v_\parallel)\lambda} d\lambda. \tag{24}$$

If we then let $\hat{\phi}_{l,m}[\epsilon(t-\lambda)] \approx \hat{\phi}_{l,m}(\epsilon t) e^{-\epsilon\lambda\gamma_{l,m}}$ (an assumption appropriate both for the Landau-damped normal modes

and the drift modes, where $\gamma_{l,m}$ is the damping/growth rate which we assume occurs on the slow time scale), we obtain (after some algebra) the linear expression

$$\widehat{\delta f}_{\alpha,l,m}(v_\parallel,\epsilon t)=\frac{mF_{0\alpha}(v_\parallel)\left(\omega_N^*+\frac{q_\alpha}{q_i}k_\parallel v_\parallel\right)\hat{\phi}_{l,m}(\epsilon t)}{\omega_{l,m}-mk_\parallel v_\parallel+i\epsilon\gamma_{l,m}}. \tag{25}$$

Here, it is notable that the modes for which $m=0$ (zonal flows) are strictly nonlinearly generated. For all other modes, we can use Eq. (25) to find the linear dispersion relation

$$0=k_\perp^2(l,m)-\sum_\alpha\left(1+\frac{mq_\alpha}{q_i}\frac{\omega_N^*}{\omega_{l,m}+i\epsilon\gamma_{l,m}}\right)\times\int_{-\infty}^{\infty}\frac{mk_\parallel v_\parallel F_{0\alpha}(v_\parallel)}{\omega_{l,m}-mk_\parallel v_\parallel+i\epsilon\gamma_{l,m}}dv_\parallel. \tag{26}$$

From the latter equation we can recover the drift wave by assuming that the resonant phase velocity is much larger than the ion thermal speed (so that ion terms may be neglected altogether) and much less than the electron thermal speed; expansion in powers of ϵ then yields

$$0=k_\perp^2(l,m)+1-\frac{m\omega_N^*}{\omega_{l,m}}+\frac{m\omega_N^*i\epsilon\gamma_{l,m}}{\omega_{l,m}^2}+\frac{i\sqrt{\pi}(\omega_{l,m}-m\omega_N^*)\sigma}{\sqrt{2}mk_\parallel v_{te}} \tag{27}$$

with $\sigma=\mathrm{sign}(\gamma_{l,m}/m)$ and solution

$$\omega_{l,m}=\frac{m\omega_N^*}{1+k_\perp^2(l,m)};\quad \epsilon\gamma_{l,m}=\frac{\sqrt{\pi}\omega_N^{*2}k_\perp^2(l,m)m\sigma}{[1+k_\perp^2(l,m)]^3\sqrt{2}k_\parallel v_{te}}. \tag{28}$$

One observes that $\omega_{l,m}=-\omega_{l,-m}=-\omega_{-l,-m}$ and that the drift modes grow (or damp) independently of the sign of l or m. Consequently, Eq. (25) can be used to show that $\hat{\phi}_{l,-m}^*(\epsilon t)=\hat{\phi}_{l,m}(\epsilon t)$.

B. Nonlinear saturation

Because of the nonlinear terms in Eq. (22), the drift waves described by Eq. (26) that grow in time will eventually saturate. We can examine this saturation mechanism in a simple case by restricting the potential to modes of one particular wave number ($l=\pm1, m=\pm1$) and ignoring the parallel velocity nonlinearity [the velocity derivatives in Eq. (22)]. Our approach is very similar to the mode coupling calculation of Lee *et al.*,[22] though the latter work does not clearly distinguish the separate time scales in the problem (and thus yields the scaling of the saturation level only up to a numerical coefficient); a similar derivation valid in the one-dimensional case has been carried out by Parker and Lee.[17] The equation for $(l=2,m=0)$ is given by

$$\frac{\partial}{\partial t}\delta f_{\alpha,2,0}(v_\parallel,\epsilon t)-i\omega_{2,0}\delta f_{\alpha,2,0}(v_\parallel,\epsilon t)+2\epsilon k_xk_ye^{i\omega_{2,0}t}\left[\hat{\phi}_{1,1}(\epsilon t)\widehat{\delta f}_{\alpha,1,-1}(v_\parallel,\epsilon t)-\hat{\phi}_{1,-1}(\epsilon t)\widehat{\delta f}_{\alpha,1,1}(v_\parallel,\epsilon t)\right]=0, \tag{29}$$

which forces $\omega_{2,0}=0$. Substitution of the linear values for $\widehat{\delta f}_{\alpha,1,\pm1}(v_\parallel,\epsilon t)$ then yields the nonlinear result

$$\widehat{\delta f}_{\alpha,2,0}(v_\parallel,\epsilon t)=-\frac{2i\epsilon k_xk_yF_{0\alpha}(v_\parallel)\hat{\phi}_{1,1}(\epsilon t)\hat{\phi}_{1,-1}(\epsilon t)}{(\omega_{1,1}-k_\parallel v_\parallel)^2+\epsilon^2\gamma_{1,1}^2}\times\left(\omega_N^*+\frac{q_\alpha}{q_i}k_\parallel v_\parallel\right). \tag{30}$$

A similar procedure for $l=0,m=2$ yields no contribution, so we can then write the nonlinear equation for $(l=1,m=1)$;

$$\frac{\partial}{\partial t}\widehat{\delta f}_{\alpha,1,1}(v_\parallel,\epsilon t)-i(\omega_{1,1}-k_\parallel v_\parallel)\widehat{\delta f}_{\alpha,1,1}(v_\parallel,\epsilon t)+i\hat{\phi}_{1,1}(\epsilon t)F_{0\alpha}(v_\parallel)\left(\omega_N^*+\frac{q_\alpha}{q_i}k_\parallel v_\parallel\right)+2\epsilon k_xk_y\hat{\phi}_{1,-1}^*(\epsilon t)\widehat{\delta f}_{\alpha,2,0}(v_\parallel,\epsilon t)=0 \tag{31}$$

with approximate solution

$$\widehat{\delta f}_{\alpha,1,1}^{NL}=\frac{F_{0\alpha}(v_\parallel)\left(\omega_N^*+\frac{q_\alpha}{q_i}k_\parallel v_\parallel\right)\hat{\phi}_{1,1}(\epsilon t)}{\omega_{1,1}-k_\parallel v_\parallel+i\epsilon\gamma_{1,1}}\cdot\left[1-\frac{4\epsilon^2k_x^2k_y^2|\hat{\phi}_{1,-1}(\epsilon t)|^2}{(\omega_{1,1}-k_\parallel v_\parallel-i\epsilon\gamma_{1,1})(\omega_{1,1}-k_\parallel v_\parallel+3i\epsilon\gamma_{1,1})}\right]. \tag{32}$$

When this result is inserted into the Poisson equation and the drift-wave dispersion relation calculated, we obtain

$$0=k_\perp^2(1,1)+1-\frac{\omega_N^*}{\omega_{1,1}^{NL}}+i\frac{\omega_N^*\epsilon}{\omega_{1,1}^2}\left(\gamma_{1,1}^{NL}-\gamma_{1,1}\left[1-\frac{k_x^2k_y^2|\hat{\phi}_{1,-1}(\epsilon t)|^2e^{-\delta^2}}{\gamma_{1,1}^2}\right]\right), \tag{33}$$

where $\delta\equiv\omega_{1,1}/\sqrt{2}k_\parallel v_{te}$. The real part of the frequency is unchanged, but saturation occurs when the potential grows such that the imaginary term is zero;

$$|\hat{\phi}_{1,\pm1}(\epsilon t)|\approx\frac{\gamma_{1,1}e^{\delta^2/2}}{k_xk_y} \tag{34}$$

(note that $\hat{\phi}_{1,1}=\hat{\phi}_{1,-1}^*$), which predicts a saturation level higher by a factor of $2e^{\delta^2/2}\approx2$ than the calculation of Ref. 22. Comparing this result with our simulations, we find that this procedure gives a quite reasonable estimate for the saturation level, as Fig. 4 shows. The difference between our calculation and the calculation of Ref. 22 lies in the treatment of the separate time scales corresponding to mode oscillation and mode growth; if these time scales are reasonably well separated, a more careful treatment of the

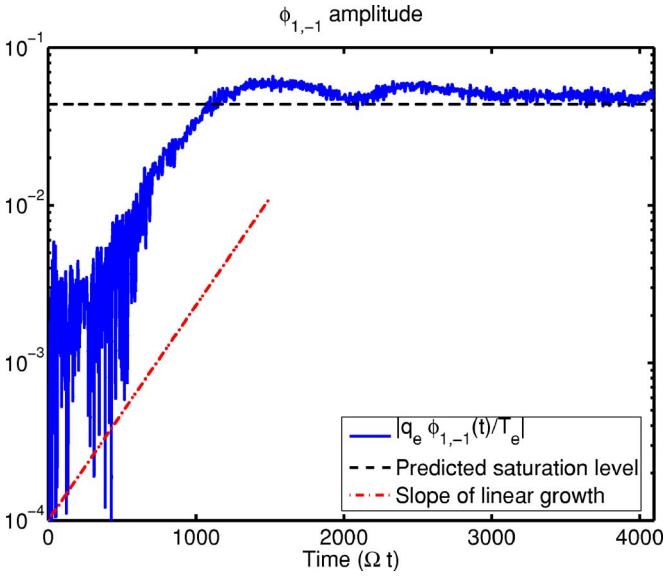

FIG. 4. (Color online) The nonlinearly saturated $\phi_{1,-1}(t)$ mode amplitude and the quasilinear prediction of Eq. (34) for the saturation level, together with the expected growth rate from linear theory (only the slope of the line is meaningful). The simulation uses the same parameters as Fig. 3.

numerical coefficient multiplying the $\gamma/k_x k_y$ scaling (predicted by the earlier calculation) can be obtained. In any case, one can plausibly argue (both analytically and from the data) that nonlinear effects do indeed cause the mode to saturate, and it is the existence of such a saturation mechanism (rather than the detailed description of it) that we will primarily make use of in the remainder of this paper.

V. SATURATED STATES AND THE FDT

If we include a density gradient in the background distribution, the dielectric function in Eq. (3) generalizes to

$$\mathcal{D}_{l,m}(\omega) = 1 + \frac{X_i}{k_\perp^2(l,m)}\left(1 + \frac{m\omega_N^*}{\omega}\right) + \frac{X_e}{k_\perp^2(l,m)}\left(1 - \frac{m\omega_N^*}{\omega}\right). \tag{35}$$

The introduction of a density gradient as a free-energy source necessarily implies that the system is no longer in thermal equilibrium, so one cannot apply the fluctuation-dissipation theorem directly without careful consideration. It is plausible, however, that the theorem can be applied to a nonlinearly saturated system containing only damped and marginally stable modes when the deviation from thermal equilibrium is small (note that this would not include systems wherein nonlinear phenomena, such as Compton scattering, transfer fluctuation energy from waves that continually grow). For the nonlinearly saturated drift waves we have simulated, we know from Eq. (28) that the real frequency of the drift wave, which scales as ω_N^* and arises from the interaction of the density gradient and the low-frequency ion acoustic wave, is well separated from the high-frequency components of the fluctuation spectrum. Even when the background gradient is large enough to amplify these low-frequency fluctuations and produce unstable drift waves, our simple model for the saturation mechanism predicts a negligible shift in the real frequency of the mode. Low-frequency fluctuations are amplified by the density gradient, grow, and nonlinearly saturate, but their energy remains in the low-frequency portion of the spectrum (as demonstrated in the previous section), well separated from and having negligible effects on the high-frequency modes where the bulk of the discreteness-induced noise resides. Consequently, it remains feasible to use the FDT to predict the behavior of the high-frequency portion of the spectrum.

As before, we can find the ω_H modes by taking the limit of the dielectric function as $\xi_e, \xi_i \gg 1$, obtaining

$$\mathcal{D}_{l,m}(\omega) \approx 1 - \frac{\omega_H^2}{\omega^2} + \frac{m\omega_N^*\omega_H^2}{\omega^3}; \quad \omega_H^2 \approx \frac{k_\parallel^2 m^2 v_{te}^2}{k_\perp^2(l,m)}. \tag{36}$$

Because we assume ω_N^* is small, its effect on the ω_H modes is slight; to lowest order, we can neglect it and recover the result of Eq. (10). Integrating the latter result only over the high frequencies, we see that the fluctuation energy in the normal modes should continue to scale inversely as the number of particles [as in Eq. (14)].

If we attempt to apply Eq. (8) to the portion of the spectrum containing the drift wave, the dispersion relation (assuming a nonlinear saturation of the general form described previously) is given by

$$\mathcal{D}_{l,m}(\omega) \approx \frac{1 + k_\perp^2(l,m)}{k_\perp^2(l,m)}\left(1 - \frac{\omega_{l,m}}{\omega} + i\frac{\omega_{l,m}\delta_s}{\omega^2}\right), \tag{37}$$

where δ_s goes to zero as the system saturates nonlinearly and $\omega_{l,m}$ is given by Eq. (28). In this case, Eq. (8) suggests that for the drift waves,

$$\langle \delta\phi\delta\phi\rangle_{l,m}(\omega)|_{\text{small }\omega} = \frac{2\pi}{N[1 + k_\perp^2(l,m)]}\delta(\omega - \omega_{l,m}). \tag{38}$$

Because drift waves arise from the destabilization of ion acoustic waves by a density gradient, the resemblance of this equation to Eq. (12) is not surprising. Although additional physical effects (the linear growth and saturation of the drift modes) have arisen that the thermal equilibrium FDT (and thus, the latter equation) does not capture, our simulation results (later in this section) suggest that the prediction of Eq. (12) regarding the scaling of the low-frequency discrete particle noise with N has relevance in the presence of the drift wave as well, as the noise does not appear to be amplified by the linear mode growth. A simple estimate of the low-frequency discreteness-induced fluctuation level [the square root of the frequency integral of Eq. (38)] yields a much smaller amplitude (on the order of 3% for typical simulation parameters used in this section) than the quasilinear saturation level of Eq. (34). The attainment of a nonlinearly saturated steady state by the drift wave suggests that it may be of interest to determine whether more general equations [akin to Eqs. (10) and (38)] can be constructed to describe low-frequency discreteness-induced fluctuations about this steady state. A brief discussion on the possibility of developing an FDT for nonthermal equilibria is presented in Ref. 28; the effects of discreteness-induced noise in such plasmas are also addressed heuristically by Kadomtsev.[29] Although we do not

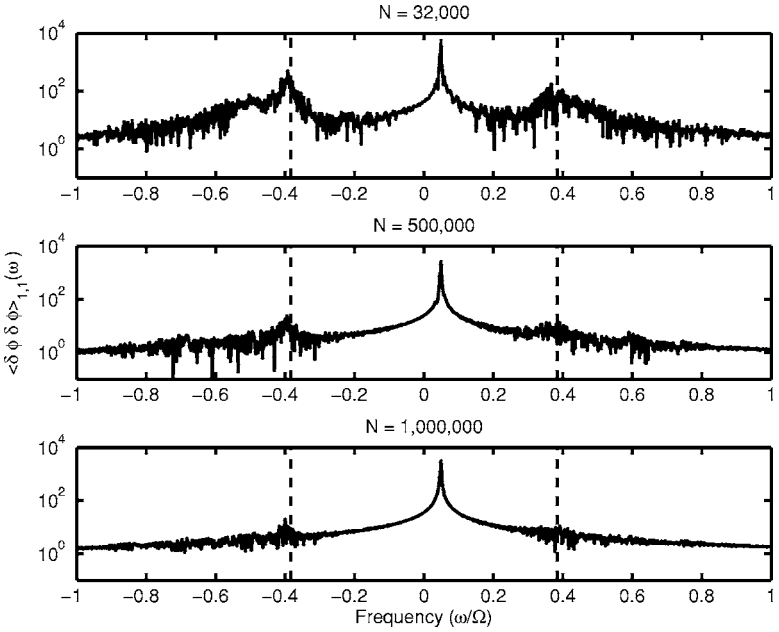

FIG. 5. As the number of particles in the simulation is increased, the saturation amplitude of the drift wave remains constant while the amplitude of the spectral noise carried by the ω_H modes (whose real frequencies are indicated by dashed lines) decreases.

pursue it here, the possibility of obtaining further information about the noise by calculating fluctuations about a nonlinearly saturated steady state is potentially interesting.

Turning to our data, we observe that the physical process described by the numerically obtained spectrum is not merely fluctuations at the real frequency of the drift wave, but the nonlinear saturation of these fluctuations as they are amplified by the density gradient. This saturation amplitude must be independent of the number of markers if the code has converged; thus, we should expect the fluctuation spectrum to exhibit a large peak at $\omega=\omega_{l,m}$ with amplitude independent of N. As well, the spectrum should contain peaks at the normal mode frequencies $\omega=\pm\omega_H$ with amplitudes that decrease inversely with N. Figure 5 confirms that this is indeed the case; these simulations use $\omega_N^*=0.055$ and $\Delta t=0.125$ while varying the particle count ($N=[3.2\times10^4, 5.0\times10^5, 1.0\times10^6]$). The other system parameters are given by $L_x=L_y=23$, $\theta=0.01$, $v_{te}^2=1837.0$, and $T_e/T_i=1$ (as in Fig. 3). It should be mentioned here that the spatially averaged δf_α is much smaller than the equilibrium distribution function $F_{0\alpha}$ near the phase velocity of the wave; we show this effect in Fig. 6 for the electrons. Thus, the deviation from equilibrium in the steady state is indeed small.

Some insight into the effects of discrete particle noise can be obtained by studying the behavior of Fig. 5 as the damping rate of the normal modes increases (this can be done by reducing the size of the slab in the y direction). As we have previously noted, the concept of "normal modes" is not well-defined for large damping rate. As random fluctuations Landau damp away on time scales increasingly near the period of the real oscillation of the "wave," the energy in these fluctuations begins to spread from a single real fre-

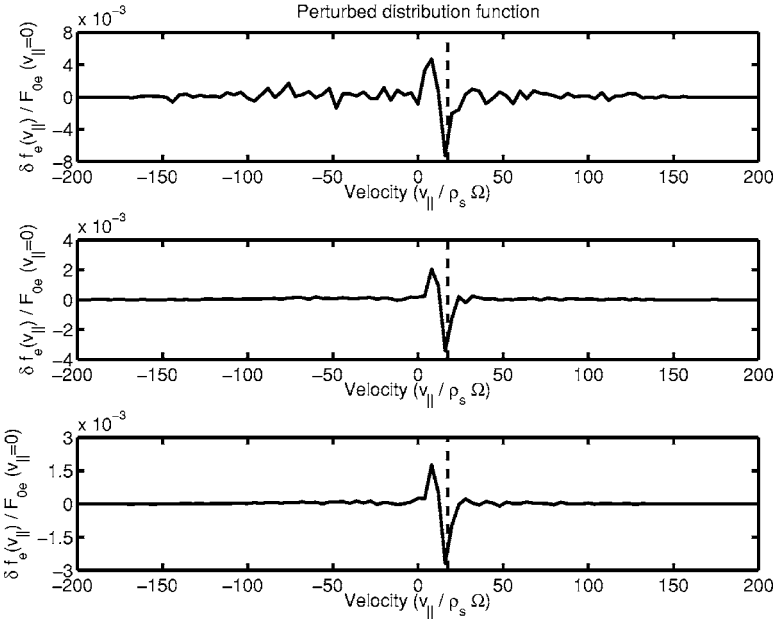

FIG. 6. The spatial average of the perturbed distribution function δf_e, normalized to the value $F_{0e}(v_\parallel=0)$ (where F_{0e} is the background Maxwellian) for the three simulations of Fig. 5. The resonant phase velocity of the drift wave is indicated by the dashed lines.

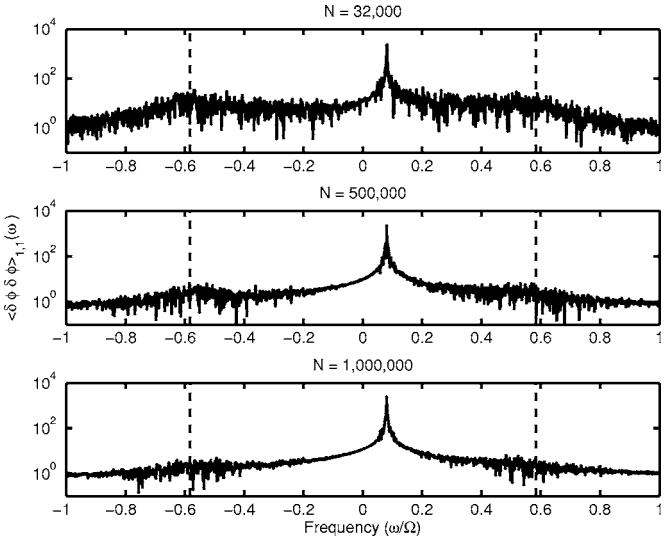

FIG. 7. In the absence of clearly defined normal modes (with the real frequency of the strongly damped ω_H mode indicated by dashed lines), the broad spectrum of background noise overlaps the portion of the spectrum occupied by the growing drift wave at low N. Nevertheless, the noise amplitude does not appreciably affect the saturation amplitude of this wave, and favorable scaling of the noise amplitude is obtained as the particle count is raised.

quency (that of the original normal mode) to a broadband in frequency space, essentially creating a background of incoherent noise for modes of a given wavelength. Running simulations to investigate the effects of this broad-spectrum noise, we find that even when the normal modes of a system are not well-defined, the fluctuation spectrum still predicts the correct saturation amplitude (independent of particle count) for the drift wave while preserving the favorable scaling of the noise with particle count across the remainder of the spectrum. Figure 7 shows this effect; for these simulations, we have set $L_y=12$ and left the other system parameters unchanged from Fig. 5. It is noteworthy that while the normal mode fluctuations are well-separated from the growing drift mode in the spectra of Fig. 5, the broad, noisy band of discreteness-induced fluctuations in the top portion of Fig. 7 has spread to encompass the frequency of the drift mode (because of the low particle count). Nevertheless, this overlapping (in frequency space) of incoherent noise and (small-amplitude) coherent drift fluctuations has no appreciable effect on the saturation amplitude of the drift mode; the amplitude remains constant as the increasing particle count reduces the discrete particle noise at the drift frequency to negligible values. One might wonder about the validity of this result if the saturation amplitude were much lower than the amplitude of the incoherent noise; such a case might arise for weakly unstable drift modes [recall that the saturation amplitude scales as the growth rate, as in Eq. (34)]. However, in particle simulations the amplitude of the noise can always be reduced by using more simulation particles, and convergence studies can be used to discern when the contribution of the noise has become negligible. For these long-wavelength modes, and in the absence of mode coupling, this condition is well satisfied when the number of markers used is on the order of 30 particles per species per grid cell (the middle graphs of Figs. 5 and 7). In general, the inclusion of mode coupling effects will increase the number of particles per cell needed to guarantee convergence, and we address this issue below. Geometrical effects (e.g., the transition from slab to toroidal geometry) may also play a role, though a thorough treatment of that issue is beyond the scope of this work.

Because we have only retained the $(\pm 1,\pm 1)$ Fourier components of the potential in our earlier simulations (effectively removing coupling terms between short-wavelength and long-wavelength modes), it is of interest to assess the effects of mode coupling on our conclusions. In general, we find that the long-term behavior of the saturated drift modes we have considered is not substantially affected by the presence of shorter-wavelength modes in the system. We consider an elongated slab with simulation parameters $L_x=95.0, L_y=9.5, \theta=0.01, v_{te}^2=1837.0, T_e/T_i=1$, and $\omega_N^*=0.043$ with $N=10\,000\,000$ particles and $N_x\times N_y=128\times 32$ grid points, and use the four-point averaging method of Ref. 30 to retain full gyroradius effects, allowing in this system all modes with $k_\perp\rho_i\leq\sqrt{2}$. This elongated geometry bears some resemblance to experimentally observed plasmas in tokamaks, with variation in x and y corresponding to radial and poloidal variation [and the $(0,1)$ mode we study corresponding to a radial streamer]. As shown in Fig. 8, although the initial growth rate is affected somewhat by the presence of other modes, the saturation amplitude of the $(0,1)$ mode remains consistent, and its long-time behavior is not substantially affected.[31] Though the signal is noisier when more modes are retained, this can be easily dealt with by using more particles in the simulation; we observe that the root-mean-square deviation of the potential from its running average (over an interval $T_{\rm av}=500\Delta t$) increases by roughly a factor of 2 for typical parameters when mode coupling effects are included. Consequently, increasing the number of markers by a factor of 4 (relative to the case where mode coupling is absent and the simulation has converged) is generally sufficient to compensate for the increased noise associated with mode coupling in these simulations of slowly growing drift modes.

VI. CONCLUSIONS

We have shown that when the normal modes (ω_H modes) of the gyrokinetic plasma are well-defined, the fluctuation energy carried by these modes scales inversely as the number of simulation particles even in the presence of saturated low-frequency drift instabilities. Although such instabilities are driven when the plasma is not in thermal equilibrium, one may nevertheless appeal to the fluctuation-dissipation theorem to plausibly explain this effect; the power in the fluctuation spectrum (in thermal equilibrium) is contained in high-frequency normal mode fluctuations, but the introduction of a mild density gradient significantly affects fluctuations only at frequencies substantially lower than those of the normal modes. These fluctuations are amplified (by the free energy of the background gradient) until they saturate nonlinearly, maintaining the plasma in a marginally stable, nonequilibrium state.

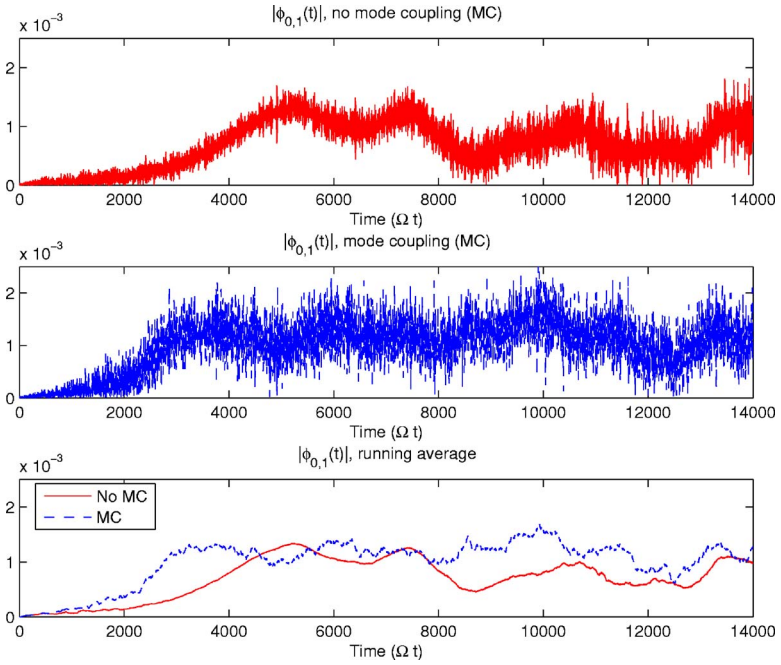

FIG. 8. (Color online) The long-time behavior of $\phi_{0,1}(t)$ is shown for an elongated simulation with $L_x=95.0, L_y=9.5$. Only the $(0,\pm1)$ components of the potential have been retained in the top curve; the simulation shown in the middle plot retains all the modes for which $k_\perp\rho_i<\sqrt{2}$. A running average over several periods of the high-frequency noise is taken below, showing that mode coupling has no effect on the initial saturation level and little effect on the long-time behavior of the saturated drift mode.

Interestingly, the favorable scaling (with particle count) of the fluctuation energy external to the drift wave is preserved even when the normal modes are not well-defined and are replaced by a broad spectrum of incoherent, particle-discreteness-induced noise not well separated from the drift wave. Further, the saturation and long-time behavior of the saturated drift modes is not substantially affected by mode coupling, and fairly modest simulation parameters are sufficient to adequately curtail the effects of discrete particle noise of these waves when the long-term state of the plasma contains only damped or marginally stable modes. We believe that the degree to which the latter result holds true in more general situations is a question meriting further study, and that the present work demonstrates the importance of including the self-consistent plasma response when assessing the effects of discrete particle noise in PIC simulations.

ACKNOWLEDGMENTS

One of us (T.G.J.) would like to acknowledge useful discussions with Dr. John Krommes. We also appreciate the referee's helpful comments regarding the manuscript.

This work is supported by U.S. Department of Energy Contract No. DE-AC02-76-CHO-3073 and the SciDAC Center for Gyrokinetic Particle Simulations of Turbulent Transport in Burning Plasmas.

[1] P. Rutherford and E. A. Frieman, Phys. Fluids **11**, 569 (1968).
[2] J. B. Taylor and R. J. Hastie, Plasma Phys. **10**, 479 (1968).
[3] W. W. Lee, Phys. Fluids **26**, 556 (1983).
[4] W. W. Lee, J. Comput. Phys. **72**, 243 (1987).
[5] W. W. Lee, S. Ethier, W. X. Wang, W. M. Tang, and S. Klasky, J. Phys.: Conf. Ser. **46**, 73 (2006).
[6] W. X. Wang, Z. Lin, W. M. Tang, W. W. Lee, S. Ethier, J. L. V. Lewandowski, G. Rewoldt, T. S. Hahm, and J. Manickam, Phys. Plasmas **13**, 092505 (2006).
[7] W. Wan, Y. Chen, and S. E. Parker, Phys. Plasmas **12**, 012311 (2005).
[8] Y. Chen and S. E. Parker, Phys. Plasmas **8**, 2095 (2001).
[9] Z. Lin, T. S. Hahm, W. W. Lee, W. M. Tang, and R. B. White, Phys. Plasmas **7**, 1857 (2000).
[10] S. E. Parker, W. W. Lee, and R. A. Santoro, Phys. Rev. Lett. **71**, 2042 (1993).
[11] Z. Lin, S. Ethier, T. S. Hahm, and W. M. Tang, Phys. Rev. Lett. **88**, 195004 (2002).
[12] W. M. Nevins, G. W. Hammett, A. M. Dimits, W. Dorland, and D. E. Shumaker, Phys. Plasmas **12**, 122305 (2005).
[13] Z. Lin, L. Chen, and F. Zonca, Phys. Plasmas **12**, 056125 (2005).
[14] G. Hu and J. A. Krommes, Phys. Plasmas **1**, 863 (1994).
[15] A. Y. Aydemir, Phys. Plasmas **1**, 822 (1994).
[16] A. B. Langdon and C. K. Birdsall, Phys. Fluids **13**, 2115 (1970).
[17] S. E. Parker and W. W. Lee, Phys. Fluids B **5**, 77 (1993).
[18] W. W. Lee, J. L. V. Lewandowski, T. S. Hahm, and Z. Lin, Phys. Plasmas **8**, 4435 (2001).
[19] J. A. Krommes, W. W. Lee, and C. Oberman, Phys. Fluids **29**, 2421 (1986).
[20] A. B. Langdon, Phys. Fluids **22**, 163 (1979).
[21] C. K. Birdsall and A. B. Langdon, *Plasma Physics via Computer Simulation* (McGraw-Hill, New York, 1985).
[22] W. W. Lee, J. A. Krommes, C. R. Oberman, and R. A. Smith, Phys. Fluids **27**, 2652 (1984).
[23] J. A. Krommes, Phys. Fluids B **5**, 1066 (1993).
[24] Y. L. Klimontovoch, *The Statistical Theory of Non-Equilibrium Processes in a Plasma* (MIT Press, Cambridge, MA, 1967).
[25] I. Manuilskiy and W. W. Lee, Phys. Plasmas **7**, 1381 (2000).
[26] J. A. Krommes and G. Hu, Phys. Plasmas **1**, 3211 (1994).
[27] A. N. Kaufman, J. Plasma Phys. **8**, 1 (1972).
[28] G. Bekefi, *Radiation Processes in Plasmas* (Wiley, New York, 1966), pp. 126–130.
[29] B. B. Kadomtsev, *Plasma Turbulence* (Academic, London, 1965), pp. 44–46.
[30] W. W. Lee and H. Qin, Phys. Plasmas **10**, 3196 (2003).
[31] As has been noted by several authors, the mean-square weight in a collisionless PIC simulation grows monotonically in time, leading to inaccuracy if simulations are run indefinitely. However, the relevant time scale for this phenomenon considerably exceeds the period of any dataset in this work, as the variation of $\langle w^2\rangle$ over the course of our simulations is generally quite small.